https://doi.org/10.15407/ujpe68.5.318

M.P. GORISHNYI

Department of Molecular Photoelectronics, Institute of Physics, Nat. Acad. of Sci. of Ukraine
(46 Nauky Ave., Kyiv, 03028, Ukraine; e-mail: miron.gorishny@gmail.com)

SURFACE MORPHOLOGY OF THE FILMS OF THE C_{60}/C_{70} FULLERENE MIXTURE. IDENTIFICATION OF C_{60} AND C_{70} IN THE C_{60}/C_{70} FILMS USING ABSORPTION SPECTRA

Films of the C_{60}/C_{70} mixture are deposited onto various substrates in a vacuum of 6.5 mPa using the thermal sublimation method. The surface morphology of 195-nm C_{60}/C_{70} films is studied. It is found that polycrystalline and quasi-amorphous C_{60}/C_{70} films are formed on silica and copper substrates, respectively. The nature of the C_{60} and C_{70} absorption bands has been discussed in detail by analyzing the literature and our data. The absorption spectra of the C_{60} and C_{70} films and the C_{60}/C_{70} mixture films are described as the sum of Gaussian functions. The absorption bands of C_{60} (at 2.474, 3.440, and 3.640 eV) and C_{70} (at 2.594, 2.804, 3.018, and 3.252 eV) can be used to identify those substances in fullerene mixtures. C_{60} is found to be the dominant component in the C_{60}/C_{70} films.

Keywords: thin film, surface morphology, absorption spectra, fitting, Gaussians, C_{60}/C_{70} mixture.

1. Introduction

The C_{60} and C_{70} fullerenes were discovered in 1985 [1]. A molecular quasi-spherical cluster C_{60} is formed by 12 pentagonal and 20 hexagonal faces with 60 carbon atoms at their vertices. Such a cluster is described by the point symmetry group I_h. A molecular cluster C_{70} has a quasi-ellipsoidal shape owing to additional 5 hexagonal faces along the equatorial line, and it is described by the point symmetry group D_{5h} [2].

C_{60} and C_{70} materials are widely used as electron acceptors in organic solar cells [3]. C_{60} was applied in solar cells [4], photovoltaic devices [5], photocatalysts [6], phototherapy [7], and biosensors [8]. C_{70} is suitable for replacing C_{60} in organic solar cells. For instance, the light conversion efficiency η in bulk heterojunctions was 2.87% in the C_{70}/zinc phthalocyanine (ZnPc) heterojunction and 2.27% in the C_{60}/ZnPc one. The larger value of η is a result of the stronger light absorption by C_{70} in a spectral interval of 1.771–2.480 nm [9]. The optical absorption spectra of "pure" C_{60} (99.86% purity) and C_{70} (>99% purity) were registered in n-hexane at room temperature [10].

In work [10], C_{60} and C_{70} were obtained using the method of Krätschmer *et al.* [11]. Then they were extracted from the benzene solution of initial graphite soot and purified using the column chromatography method.

The optical absorption spectra of C_{60} in n-hexane solutions and the nature of their bands were studied in work [12]. The optical absorption spectra of the C_{60} and C_{70} films were studied in works [11, 13, 14] and [15], respectively. It was found that the absorption bands of the C_{60} and C_{70} films are shifted to the red with respect to the corresponding bands in the spectra of their solutions, which is a result of the intermolecular interaction in the solid state.

A review of the most important theoretical and experimental papers aimed at elucidating the properties of the lowest excited states in C_{60} and C_{70} was made in work [16]. The diagrams of the energy levels of the C_{60} and C_{70} molecules were given in works [2, 14, 17–21].

Citation: Gorishnyi M.P. Surface morphology of the films of the C_{60}/C_{70} fullerene mixture. Identification of C_{60} and C_{70} in the C_{60}/C_{70} films using absorption spectra. *Ukr. J. Phys.* **68**, No. 5, 318 (2023). https://doi.org/10.15407/ujpe68.5.318.
Цитування: Горішний М.П. Морфологія поверхні плівок суміші фулеренів C_{60}/C_{70}. Ідентифікація C_{60} та C_{70} у плівках C_{60}/C_{70} за їх спектрами поглинання. *Укр. фіз. журн.* **68**, №5, 318 (2023).

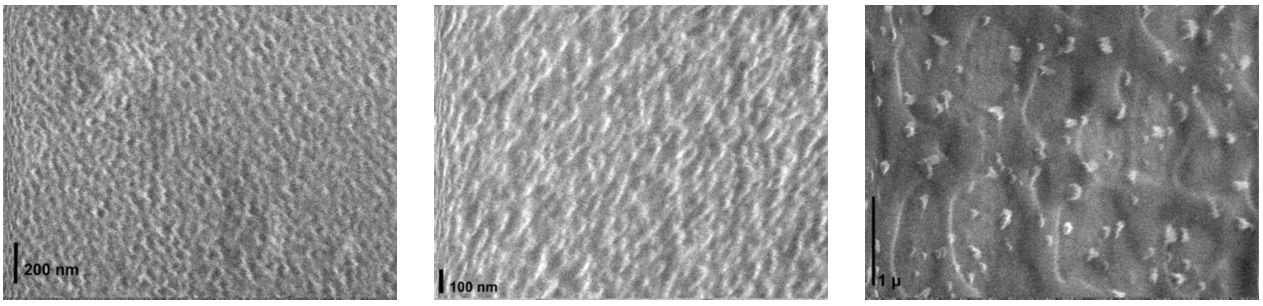

a *b* *c*

Fig. 1. SEM micrographs of 195-nm C_{60}/C_{70} films deposited in vacuum on silica substrates with thin carbon (*a*) and ITO (*b*) layers, and on a copper substrate (*c*)

According to the mass spectrometry data [10], when the fullerenes are synthesized, molecules with various numbers of carbon atoms are formed. They are described by the general formula C_{2n}, where the natural number n varies from 26 to 35. The most stable components of this mixture are the C_{60} and C_{70} molecules. Therefore, the study of the absorption spectra of the solutions and films of pure C_{60} and C_{70} substances is a challenging task for their identification in solid mixtures of synthesized fullerenes.

In this work, the surface morphology of the C_{60}/C_{70} films and the nature of the absorption bands of C_{60} and C_{70} in the molecular and solid states are studied in order to identify those substances by their bands in the absorption spectra of the films of C_{60}/C_{70} mixtures.

2. Specimen Preparation and Experimental Technique

In our research, we used a mixture of fullerenes (MER Corporation) with the following composition: 76% C_{60}, 22% C_{70}, and 2% higher-order fullerenes. Hereafter, this mixture will be denoted by C_{60}/C_{70} according to its main components.

To study their optical absorption properties, thin C_{60}/C_{70} films with various thicknesses d within an interval of 25–195 nm were deposited onto silica substrates in a vacuum of 6.5 mPa using the thermal sublimation method. The initial C_{60}/C_{70} mixture was sublimated from a ceramic crucible heated up by passing an electric current through a nichrome spiral. During the sputtering process, the temperature of the ceramic crucible varied from 673 to 723 K; it was measured with the help of a chromel-alumel thermocouple.

The start and final moments of the film deposition were registered using a thickness gauge MSV-1841. The film thickness was measured by means of an interference thickness gauge MII-4.

The absorption spectra of thin C_{60}/C_{70} films within an interval of 1.305–4.133 eV were registered at room temperature using a Perkin Elmer Lambda 25 UV-Vis spectrophotometer with a spectral slit width of 1 nm. The absorption measurement error did not exceed 2%.

The surface morphology of C_{60}/C_{70} films deposited onto silica substrates with thin carbon or indium tin oxide (ITO) layers and onto copper substrates was studied with the help of a JSM-35 JEOL scanning electron microscope.

3. Results and Their Discussion

3.1. Surface morphology of C_{60}/C_{70} films

The surface morphology of solid 195-nm C_{60}/C_{70} films deposited in a vacuum of 6.5 mPa is shown in Fig. 1. Needle-like and round crystallites of various sizes are clearly seen in Figs. 1, *a* and 1, *b*. They were formed due to the van der Waals interaction between the C_{60} and C_{70} molecules. The carbon and ITO layers affect the orientation of needle-like crystallites. A higher orientation ability of the ITO layer (Fig. 1, *b*) is evident.

The mobility of the sublimated C_{60} and C_{70} molecules is restricted by their strong interaction with Cu atoms. In this case, a quasi-amorphous C_{60}/C_{70} layer first appears on the copper substrate surface. The fullerene molecules located on the surface of this layer interact less strongly with Cu atoms and, due to the van der Waals interaction, be-

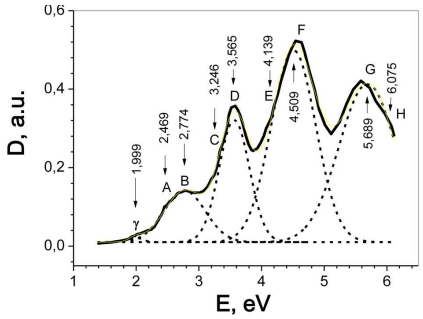

Fig. 2. Absorption spectrum of the 20-nm C_{60} film on a silica substrate at room temperature (solid curve) (taken from [9]). Fitting of this spectrum by five Gaussians (dashed curves)

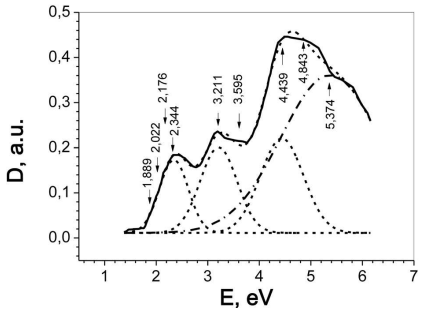

Fig. 3. Absorption spectrum of the 20-nm C_{70} film on a silica substrate at room temperature (solid curve) (taken from [9]). Fitting of this spectrum by four Gaussians (dashed curves)

come the formation centers of rounded crystallites at various places of the quasi-amorphous layer surface (Fig. 1, *c*).

The size of crystallites on all three substrates varies from 50 to 200 nm.

The SEM micrographs (Fig. 1) demonstrate the influence of the interaction between the fullerenes and the substrates on the structure of C_{60}/C_{70} films.

3.2. Optical absorption spectra of C_{60}, C_{70}, and C_{60}/C_{70} films

In this work, the absorption spectra of the C_{60} (Fig. 2) and C_{70} (Fig. 3) films were approximated by the sums of Gaussian functions using the Origin 8.5 software. The standard deviation was 6.2×10^{-5}, and the correlation coefficient 0.99682.

The energies of the transition in the spectra of the imaginary component ε_2 of the dielectric function of C_{60} hexane solutions (ε_2-spectra), as well as their assignments, are quoted in Table 1 (columns 2 and 3, respectively). The transition $h_u \to t_{1u}$ (band γ) is forbidden, because it occurs between antisymmetric electronic states. This transition becomes allowed because of its interaction with the corresponding symmetric molecular vibrations (the Herzberg–Teller or Jahn–Teller coupling) [22]. Allowed transitions occur between electronic states with different symmetries. The strengths of their oscillators are different. The degenerate electronic levels h_u and (h_g, g_g) correspond to the HOMO and HOMO $-$ 1 molecular orbitals, respectively.

The transition energies in the absorption spectra of C_{60} films are quoted in Table 1 (column 6) and indicated in Fig. 2. As a result of the molecular interaction in the C_{60} films, the molecular levels of excited states are split into narrow energy zones. When fitting the absorption spectrum profile of C_{60} films, the Gaussian functions for zones γ, B, D, F, and G were determined. Zones A, C, and E look like shoulders (sh) on the low-energy side of bands B, D, and F, respectively (Fig. 2). Bands C and H were observed in the absorption spectra of hexane solutions and C_{60} films, but they were absent in the ε_2-spectra of the C_{60} molecule (see Table 1, columns 2 and 3).

The transition energies in the absorption spectra of the films of C_{70} and its hexane solution are quoted in Table 2. Column 4 of this table contains data for the spectrum of the 20-nm C_{70} film (Fig. 3). They are consistent with the data of work [15] (see Table 2, column 3). The absorption peaks for C_{70} films are red-shifted with respect to the corresponding peaks for the C_{70} hexane solution [10, 23] (see Table 2, columns 1 and 2).

The energy structure of the C_{70} molecule was calculated *ab initio* in work [24] in the framework of the Hartree–Fock method. According to the results of those calculations, the energy level diagram of the C_{70} molecule was plotted in work [25]. We have analyzed those data and changed the level symmetry for some HOMO and LUMO molecular orbitals given in work [25], after comparing them with the relevant data from work [24]. So the symmetries of the HOMO $-$ 5, LUMO, and LUMO + 1 levels were changed to a_1', e_1'', and a_1'', respectively. According to work [24], the LUMO + 4 and LUMO + 5 levels have the e_2' and a_2'' symmetries, respectively, and they were used to explain the possible origin of transitions with energies $E \geq 3.605$ eV. The transitions in the C_{70} molecule are quoted in column 5 of Table 2.

The difference between the transition energies of 2.022 and 1.889 eV (Table 2, column 4) equals

Table 1. **Transition energies, oscillator strengths (in parentheses), and assignments of C_{60} absorption bands at room temperature**

Band code	ε_2-spectra of C_{60}-hexane solution [14]		Absorption spectra C_{60}-hexane solution [12]		Absorption spectrum of 20-nm C_{60} film (this work)
	E, eV	Assignment	E, eV	Assignment	E, eV
1	2	3	4	5	6
γ	1.995 (0.001)	$h_u \to t_{1u}$	1.999	$A_g \to 1T_{1g}$	1.999
A		$h_u \to t_{1g}$	3.037	$A_g \to 1T_{1u}$	2.469 (sh)
B	3.280 (0,001)	$h_u \to t_{1g}$	3.289	$A_g \to 2T_{1u}$	2.774
C			3.775	$A_g \to 3T_{1u}$	3.246 (sh)
D_1	3.580 (0.080)	h_g, $g_g \to t_{1u}$	4.065	$A_g \to 4T_{1u}$	3.565
D_2	3.732 (0,090)	h_g, $g_g \to t_{1u}$	4.350	$A_g \to 5T_{1u}$	
E	4.210 (0,040)	$h_u \to h_g$	4.832	$A_g \to 6T_{1u}$	4.139 (sh)
F	4.600 (0.490)	$h_u \to h_g$	5.452	$A_g \to 7T_{1u}$	4.509
G_1	5.437 (0.019)	h_g, $g_g \to t_{2u}$	5.876	$A_g \to 8T_{1u}$	5.689
G_2	5.730 (0.330)	h_g, $g_g \to t_{2u}$			
H			6.358	$A_g \to 9T_{1u}$	6.075 (sh)

N o t e: abbreviation sh stands for shoulder.

Table 2. **Transition energies, relative intensities (in parentheses), and assignments of C_{70} absorption bands at room temperature**

Absorption spectra of C_{70}				
Transition energies E, eV				Assignment [24, 25]
In hexane		Film		
[10]	[23]	[15]	This work	
1	2	3	4	5
	1.864 (sh)	1.890	1.889 (sh)	$e_1'' \to e_1''$ or $a_2'' \to a_1''$
1.946 (sh)	1.992 (sh)			
1.986 (sh)	1.999 (sh)			
2.033 (sh)		2.026	2.022 (sh)	$e_1'' \to e_1'' + E_1'$ or $a_2'' \to a_1'' + E_1'$
2.066 (sh)	2.066 (sh)			
2.087 (sh)		2.183	2.176 (sh)	$a_2' \to e_1''$
2.279 (sh)	2.254 (sh)	2.353	2.344	$e_2'' \to a_1''$
2.644 (sh)	2.649 (sh)	2.485		$e_1' \to a_1''$ or $a_2'' \to a_1'$
3.280 (mw)	3.280 (mw)	3.204	3.211	$e_2' \to e_1'$ or $a_2' \to e_1'$, or $a_1' \to a_1''$
3.454 (mw)	3.444 (mw)	3.416		$e_1' \to a_1'$
3.745 (mw)	3.745 (mw)	3.605	3.595 (sh)	$e_1' \to e_2'$
3.961 (w)		4.495	4.439	$a_2' \to a_2''$
5.767 (s)	5.794 (s)	5.688	5.374	$a_1' \to a_2''$

N o t e: abbreviation mw stands for mean weak, w for weak, s for strong, and sh for shoulder.

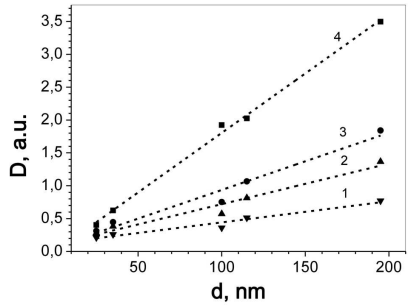

Fig. 4. Linear fitting (dashed lines) of the optical density function $D(d)$ of C_{60}/C_{70} films measured at incident photon energies of 2.412 (*1*), 2.800 (*2*), 3.196 (*3*), and 3.625 eV (*4*)

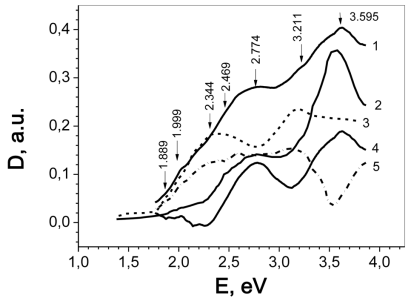

Fig. 5. Absorption spectra of films on silica substrates: (*1*) C_{60}/C_{70} mixture, $d = 25$ nm; (*2*) C_{60}, $d = 20$ nm; (*3*) C_{70}, $d = 20$ nm; (*4*) difference between curves *1* and *3*; (*5*) difference between curves *1* and *2*

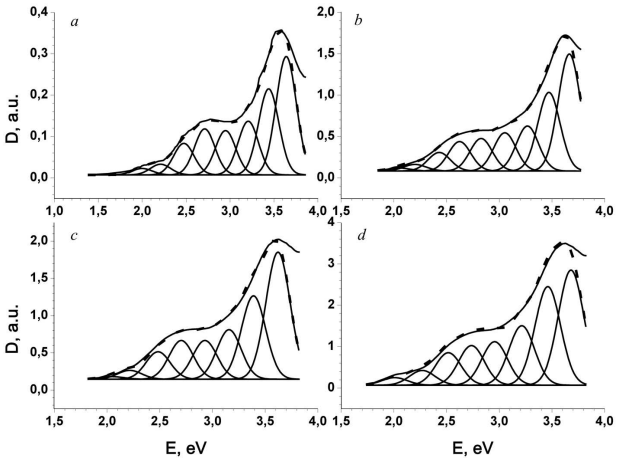

Fig. 6. Fitting of the film absorption spectra by the sums of the Gaussians with the same width (dashed curves): C_{60}, $d = 20$ nm (*a*); C_{60}/C_{70}, $d = 100$ nm (*b*); C_{60}/C_{70}, $d = 115$ nm (*c*); and C_{60}/C_{70}, $d = 195$ nm (*d*)

0.133 eV $\approx$ 1073 cm^{-1}. In work [15], the corresponding difference was found to equal 0.136 eV $\approx$ 1097 cm^{-1} (Table 2, column 3). By magnitude, those

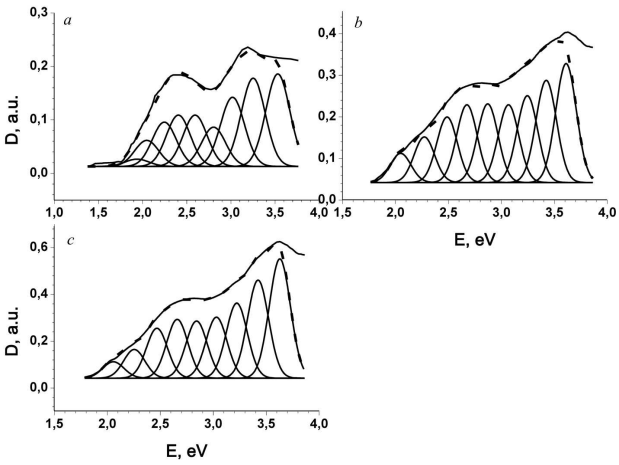

Fig. 7. Fitting of the film absorption spectra by the sums of the Gaussians with the same width (dashed curves): C_{70}, $d = 20$ nm (*a*); C_{60}/C_{70}, $d = 35$ nm (*b*); and C_{60}/C_{70}, $d = 35$ nm (*c*)

values are close to the IR frequency of C_{70} E_1' = = 1087 cm^{-1} [26]. One may assume that the absorption bands at 2.026 and 2.022 eV are a result of the interaction of the excited states e_1'' and a_1'' with the 1087-cm^{-1} vibration (the Herzberg–Teller or Jahn–Teller coupling as in the C_{60} molecule [22]). Those bands can be considered as the transitions $e_1'' \rightarrow$ $\rightarrow e_1'' + E_1'$ and $a_2'' \rightarrow a_1'' + E_1'$.

According to the Bouguer–Lambert law, we evaluated the effective absorption coefficients $\alpha(E)$ of the C_{60}/C_{70} films as the slopes of the plots $D(d)$ (Fig. 4). The values obtained for $\alpha(E)$ are 3.22×10^4 cm^{-1} for line *1*, 6.16×10^4 cm^{-1} for line *2*, 8.71×10^4 cm^{-1} for line *3*, and 1.82×10^5 cm^{-1} for line *4*. The relative measurement error of $\alpha(E)$ did not exceed 12%. Smaller relative measurement errors were obtained for larger $\alpha(E)$. The smallest error was for an incident photon energy of 3.625 eV (line *4*) and amounted to 2%. The $\alpha(E)$-values calculated from the absorption spectra of the C_{60} and C_{70} films with $d = 20$ nm for photon energies of 2.412, 2.800, 3.196, and 3.625 eV are as follows: 3.8×10^4, 6.7×10^4, 8.1×10^4, and 1.7×10^5 cm^{-1}, respectively, for the C_{60} films; and 8.5×10^4, 7.2×10^4, 1.1×10^5, and 1.0×10^5 cm^{-1}, respectively, for the C_{70} ones. A comparison of those data shows that the above-presented values of $\alpha(E)$ for the C_{60}/C_{70} films better correlate with the $\alpha(E)$-values calculated for the C_{60} films at the corresponding energies of incident photon. This fact means that C_{60} is the main component in the C_{60}/C_{70} films.

In an energy interval of 1.38–3.31 eV, the absorption of the C_{70} film is stronger than that of the C_{60} film (Fig. 5, curves *3* and *2*, respectively). In Fig. 5, the numbers near the arrows mean the transition energies for the C_{60} and C_{70} films, which were taken from Table 1 (column 5) and Table 2 (column 4). The C_{60} contribution (curve *4*) to the C_{60}/C_{70} absorption was calculated by subtracting the C_{70} spectrum (curve *3*) from the mixture one (curve *1*). Absorption spectrum *4* correlates with spectrum *2* of the C_{60} film. Absorption spectrum *5* characterizes the C_{70} contribution to the C_{60}/C_{70} absorption. This spectrum was obtained by subtracting spectrum *2* from spectrum *1,* and it correlates with C_{70} spectrum *3* in an interval of 1.8–3.6 eV. At the same time, the anti-correlation between the absorption spectra for the C_{60} and C_{70} films (curves *2* and *3*, respectively) was observed. Absorption spectra *4* and *5* also anti-correlate. Hence, from the above analysis of the absorption spectra shown in Fig. 5, it follows that both C_{60} and C_{70} enter the composition of the C_{60}/C_{70} film.

3.3. Identification of C_{60} and C_{70} in C_{60}/C_{70} films by absorption spectra

In an interval of 1.38–6.0 eV, the absorption spectra of the C_{60} (Fig. 2) and C_{70} (Fig. 3) films consist of wide structural bands. In Figs. 6 and 7, the structural absorption bands of the C_{60}, C_{70}, and C_{60}/C_{70} films are resolved as the sums of the Gaussian functions of the same width. It was done in order to determine the transition energies more accurately and to compare them within an interval of 1.38–3.80 eV. The fitting by Gaussians of the same width allows the structure of the absorption spectra of the C_{60}, C_{70}, and C_{60}/C_{70} films to be resolved more accurately and provides an opportunity to qualitatively reveal the composition dynamics of the C_{60}/C_{70} films with various thicknesses during the thermal sputtering of this mixture.

The absorption spectra of the C_{60}, C_{70}, and C_{60}/C_{70} films are grouped according to the similarity of their profiles. The absorption spectra of the C_{60} (d = 20 nm) and C_{60}/C_{70} (d = 100, 115, and 195 nm) films together with their fitting by the sums of Gaussian functions of the same width are shown in Fig. 6. Analogous fittings of the absorption spectra of the C_{70} (d = 20 nm) and C_{60}/C_{70} (d = 25 and 35 nm) films are depicted in Fig. 7 (panels *a*, *b*, and *c*, respectively). The relative intensity of each Gaussian was determined as the ratio A/A_0 between the area A under this Gaussian component and the total area A_0 under the absorption spectrum of the film, the latter being equal to the sum of the areas under all Gaussian components that form the spectrum.

The values of the energies and relative intensities of electronic transitions in the absorption spectra of the C_{60} and C_{60}/C_{70} films, which were determined from Fig. 6, are given in Table 3, and their counterparts determined for the C_{70} and C_{60}/C_{70} films from Fig. 7 are quoted in Table 4. The numbers in the second column (Band code) of those tables are the numbers of Gaussian components (C_{60} or C_{70}) in the absorption spectra of the C_{60}/C_{70} films with d = 25, 35, 100, 115, and 195 nm.

3.3.1. C_{60} contributions to the absorption spectra of C_{60}/C_{70} mixture films

The weak band at 2.007 eV, which was observed only in the absorption spectrum of the 195-nm C_{60}/C_{70} film (Table 3, row 1), was identified by us as band 1_C_{60} (γ-band) at 1.999 eV (Table 1, row 1).

In the absorption spectra of the C_{60}/C_{70} films with d = 100, 115, and 195 nm, there appears band 2_C_{60} at 2.209 eV (Table 3, row 3), which is absent in the absorption spectra of thin C_{60}/C_{70} films with d = 25 and 35 nm.

Band 3_C_{60} at 2.474 eV, which was identified as band A (Table 1), was observed in the absorption spectra of the C_{60}/C_{70} films of all thicknesses (Table 3, row 4; Table 4, row 5). Its relative intensity is minimum in the absorption spectrum of the 100-nm C_{60}/C_{70} film.

In the absorption spectra of the C_{60}/C_{70} films with d = 115 and 195 nm, bands 4_C_{60} and 5_C_{60} are observed; the latter at 2.712 eV (band B, Table 1) for the film thickness d = 115 nm and at 2.949 eV for d = 195 nm. The relative intensities of those bands change insignificantly with the growth of the C_{60}/C_{70} film thickness (Table 3, rows 6 and 8).

Band 6_C_{60} at 3.208 eV (band C, Table 1) is observed in the absorption spectra of the C_{60}/C_{70} films with d = 115 and 195 nm. The relative intensity of this band increases as the thickness d of the C_{60}/C_{70} film grows (Table 3, row 10).

Bands 7_C_{60} at 3.440 eV (Table 1, band D_1) and 8_C_{60} at 3.640 eV (Table 1, band D_2) are observed in the absorption spectra of all C_{60}/C_{70} films (Table 3,

Table 3. **Energies E and relative intensities A/A_0 of electronic transitions in 20-nm C_{60} films, and in 100-, 115-, and 195-nm C_{60}/C_{70} films**

No.	Band code	C_{60}, 20 nm $A_0 = 0.27799$ a.u.		C_{60}/C_{70}, 100 nm $A_0 = 1.17812$ a.u.		C_{60}/C_{70}, 115 nm $A_0 = 1.45257$ a.u.		C_{60}/C_{70}, 195 nm $A_0 = 3.00815$ a.u.	
		E, eV	A/A_0	E, eV	A/A_0	E, eV	A/A_0	E, eV	A/A_0
1	**1_C60**	1.999	0.016					2.007	0,018
2	2_C70			2.050	0.008	2.048	0.006		
3	**2_C60**	2.209	0.027	2.200	0.018	2.214	0.024	2.270	0.036
4	**3_C60**	2.474	0.079	2.431	0.050	2.484	0.073	2.517	0.079
5	5_C70			2.624	0.080				
6	**4_C60**	2.712	0.116			2.704	0.103	2.737	0.096
7	6_C70			2.828	0.088				
8	**5_C60**	2.949	0.112			2.929	0.103	2.957	0.106
9	7_C70			3.053	0.104				
10	**6_C60**	3.208	0.135			3.157	0.131	3.214	0.145
11	8_C70			3.268	0.122				
12	**7_C60**	3.440	0.216	3.472	0.213	3.389	0.222	3.461	0.240
13	**8_C60**	3.640	0.298	3.665	0.317	3.622	0.338	3.681	0.280

Table 4. **Energies E and relative intensities A/A_0 of electronic transitions in 20-nm C_{70} films, and in 25- and 35-nm C_{60}/C_{70} films**

No.	Band code	C_{70}, 20 nm $A_0 = 0.29865$ a.u.		C_{60}/C_{70}, 25 nm $A_0 = 0.39903$ a.u.		C_{60}/C_{70}, 35 nm $A_0 = 0.60292$ a.u.	
		E, eV	A/A_0	E, eV	A/A_0	E, eV	A/A_0
1	1_C70	1.936	0.016				
2	2_C70	2.047	0.055	2.049	0.043	2.057	0.029
3	3_C70	2.245	0.094	2.272	0.067	2.254	0.051
4	4_C70	2.405	0.110				
5	**3_C60**			2.487	0.096	2.468	0.088
6	5_C70	2.594	0.110	2.674	0.114	2.660	0.104
7	6_C70	2.804	0.083	2.871	0.115	2.848	0.101
8	7_C70	3.018	0.147	3.067	0.114	3.030	0.108
9	8_C70	3.252	0.188	3.245	0.127	3.222	0.133
10	**7_C60**			3.423	0.150	3.423	0.174
11	9_C70	3.531	0.197				
12	**8_C60**			3.610	0.174	3.629	0.211

rows 12 and 13; Table 4, rows 10 and 12). Their relative intensities increase with the increasing thickness of the C_{60}/C_{70} films.

The data presented above confirm the presence of the C_{60} component in the C_{60}/C_{70} films with $d = 25$, 35, 100, 115, and 195 nm. The calculated average values of the transition energies and relative intensities (in parentheses) of bands 3_C_{60}, 7_C_{60}, and 8_C_{60} in the spectra of the C_{60}/C_{70} films with all thicknesses are 2.477 eV (0.077), 2.434 eV (0.200), and 3.641 eV (0.264), respectively, and agree well with the following data obtained for the 20-nm C_{60} films: 2.474 eV (0.079), 3.440 eV (0.216), and 3.640 eV (0.298), respectively (Tables 3 and 4). Therefore, the bands at 2.474, 3.440, and 3.640 eV can be used to identify C_{60} in the fullerene mixture films by analyzing their absorption spectra. The relative variations of the energy of the C_{60} peaks at 2.474, 3.440, and

3.640 eV in the spectra of the C_{60}/C_{70} films with $d = 25$, 35, 100, 115, and 195 nm are as follows: 0.5%, −0.2%, −1.7%, 0.4%, and 1.7%, respectively, for the peak at 2.474 eV; −0.5%, −0.5%, 0.9%, −1.5%, and 0.6%, respectively, for the peak at 3.440 eV; and −0.8%, −0.3%, 0.7%, −0.5%, and 1.1%, respectively, for the peak at 3.640 eV.

3.3.2. C_{70} contributions to absorption spectra of C_{60}/C_{70} mixture films

Weak band 1_C_{70} at 1.936 eV was not observed in the absorption spectra of the C_{60}/C_{70} films (Table 4, row 1). By its position, this band is close to 1.889 eV, the energy of the transition $e''_1 \to e''_1$ or $a''_2 \to a''_1$ (Table 2).

Weak band 2_C_{70} at 2.047 eV was observed in the absorption spectra of the C_{60}/C_{70} films with $d = 25$, 35, 100, and 115 nm. The relative intensity of this band decreases as the thickness of the C_{60}/C_{70} films grows and is very low in the absorption spectra of the 100- and 115-nm C_{60}/C_{70} films (Table 4, row 2; Table 3, row 2).

The absorption spectra of the C_{60}/C_{70} films with $d = 25$ and 35 nm contain band 3_C_{70} at 2.245 eV. The relative intensity of this band decreases, as the thickness of the C_{60}/C_{70} films grows (Table 4, row 3). The maximum of this band is located in the middle between the C_{70} bands at 2.176 eV (the $a'_2 \to e''_1$ transition) and 2.344 eV (the $e''_2 \to a''_1$ transition) (Table 2).

In the absorption spectra of the C_{60}/C_{70} films, band 4_C_{70} at 2 405 eV is absent (Table 4, row 4).

Band 5_C_{70} at 2.594 eV was observed in the absorption spectra of the C_{60}/C_{70} films with $d = 25$, 35, and 100 nm. The relative intensity of this band decreases with the growth of the C_{60}/C_{70} film thickness (Table 4, row 6; Table 3, row 5). According to the position of its peak, this band is close to the C_{70} band at 2.485 eV (the transition $e'_2 \to e'_1$ or $a'_2 \to e'_1$ or $a'_1 \to a''_1$) (Table 2).

Band 6_C_{70} at 2.804 eV was observed in the absorption spectra of the C_{60}/C_{70} films with $d = 25$, 35, and 100 nm. The relative intensity of this band is maximum for the 25-nm C_{60}/C_{70} film and does not change for the 35- and 100-nm films (Table 4, row 7; Table 3, row 7).

Band 7_C_{70} at 3.018 eV was observed in the absorption spectra of the C_{60}/C_{70} films with $d = 25$, 35, and 100 nm. The relative intensity of this band decreases with the growth of the C_{60}/C_{70} film thickness (Table 4, row 8; Table 3, row 9).

Band 8_C_{70} at 3.252 eV was observed in the absorption spectra of the C_{60}/C_{70} films with $d = 25$, 35, and 100 nm. Its relative intensity does not change, as the thickness of C_{60}/C_{70} films changes (Table 4, row 9; Table 3, row 11). According to the position of its peak, this band is close to band C_{70} at 3.211 eV (the $e'_2 \to e'_1$ or $a'_2 \to e'_1$ or $a'_1 \to a''_1$ transition) (Table 2).

In the absorption spectra of the C_{60}/C_{70} films, band 9_C_{70} at 3.531 eV is absent (Table 4, row 11). We may assume that this band does not manifest itself against the background of intense C_{60} components at 3.440 and 3.640 eV. According to the position of its maximum, this band is close to the C_{70} band at 3.595 eV (the $e'_1 \to e'_2$ transition) (Table 2).

Therefore, the above data confirm the presence of the C_{70} component in the C_{60}/C_{70} films with the thicknesses $d = 25$, 35, and 100 nm. The calculated average values of the transition energies and relative intensities (in parentheses) of bands 5_C_{70}, 6_C_{70}, 7_C_{70}, and 8_C_{70} in the spectra of the C_{60}/C_{70} films with $d = 25$, 35, and 100 nm are 2.652 eV (0.099), 2.849 eV (0.101), 3.050 eV (0.109), and 3.245 eV (0.127), respectively. They agree well with the following data obtained for the 20-nm C_{70} films: 2.594 eV (0.110), 2.840 eV (0.083), 3.018 eV (0.147), and 3.252 eV (0.188), respectively (Tables 3 and 4). Therefore, the bands at 2.474, 3.440, and 3.640 eV can be used to identify C_{60} in the fullerene mixture films on the basis of their absorption spectra. The relative variations of the energy of the C_{70} peaks at 2.594, 2.804, 3.018, and 3.252 eV in the spectra of the C_{60}/C_{70} films with $d = 25$, 35, and 100 nm are as follows: 3.1%, 2.5%, and 1.2%, respectively, for the peak at 2.594 eV; 2.4%, 1.6%, and 0.8%, respectively, for the peak at 2.804 eV; 1.6%, 0.4%, and 1.1 %, respectively, for the peak at 3.018 eV; and −0.2%, −0.9%, and 0.5%, respectively, for the peak at 3.252 eV.

The variations in the relative intensities of the C_{60} and C_{70} bands in the absorption spectra of the C_{60}/C_{70} films allow us to assume that both components sublimated at the sputtering beginning, so the C_{60}/C_{70} films with the thicknesses $d \leq 100$ nm were formed via the deposition of C_{60} and C_{70} molecules onto silica substrates. The resulting films are two-component. After a drastic reduction in the intensity

of C_{70} sublimation because of a small amount of C_{70} in the crucible, the C_{60}/C_{70} films with the thicknesses $d > 100$ nm consist of two layers. The first 100-nm layer, which is in direct contact with the substrate, is two-component, whereas the next layer is single-component and mainly consists of C_{60} molecules.

4. Conclusions

The molecular interaction between the fullerenes and the substrates affects the structure of the C_{60}/C_{70} films. Polycrystalline C_{60}/C_{70} films with needle-like and round crystallites are formed on silica substrates with intermediate carbon or ITO layers. Quasi-amorphous C_{60}/C_{70} layers are formed on the surface of copper substrates, and the surface C_{60} and C_{70} molecules become centers of the crystallite formation.

The values of the effective absorption coefficient α of the C_{60}/C_{70} films are estimated for various incident photon energies E. It is found that the values of $\alpha(E)$ obtained for the C_{60}/C_{70} films correlate better with the $\alpha(E)$-values calculated for the C_{60} films and the corresponding incident photon energies. This fact means that C_{60} is the main component in the C_{60}/C_{70} films.

The nature of the C_{60} and C_{70} absorption bands is discussed in detail by analyzing the literature and our data. The C_{60} absorption bands at 2.474, 3.440, and 3.640 eV and the C_{70} absorption bands at 2.594, 2.804, 3.018, and 3.252 eV can be used to identify those substances in fullerene mixtures

The work was sponsored in the framework of the budget theme of the National Academy of Sciences of Ukraine (project No. 1.4.B/209).

1. H.W. Kroto, J.R. Heath, S.C. O'Brien, R.F. Curl, R.E. Smalley. C_{60}: buckminsterfullerene. *Nature* **318**, 162 (1985).
2. A. Graja, J.-P. Farges. Optical spectra of C_{60} and C_{70} complexes. Their similarities and differences. *Adv. Mater. Opt. Electron.* **8**, 215 (1998).
3. L. Benatto, C.F.N. Marchiori, T. Talka, M. Aramini, N.A.D. Yamamoto, S. Huotari, L.S. Roman, M. Koehler. Comparing C_{60} and C_{70} as acceptor in organic solar cells: Influence of the electronic structure and aggregation size on the photovoltaic characteristics. *Thin Solid Films.* **697**, 137827 (2020).
4. Y. Yi, V. Coropceanu, J.-L. Brédas. Exciton-dissociation and charge-recombination processes in pentacene/C_{60} solar cells: Theoretical insight into the impact of interface geometry. *J. Am. Chem. Soc.* **131**, 15777 (2009).
5. P. Brown, P.V. Kamat. Quantum dot solar cells. Electrophoretic deposition of CdSe–C_{60} composite films and capture of photogenerated electrons with nC_{60} cluster shell. *J. Am. Chem. Soc.* **130**, 8890 (2008).
6. H. Yi, D. Huang, L. Qin, G. Zeng, C. Lai, M. Cheng, S. Ye, B. Song, X. Ren, X. Guo. Selective prepared carbon nanomaterials for advanced photocatalytic application in environmental pollutant treatment and hydrogen production. *Appl. Catal. B* **239,** 408 (2018).
7. P. Mroz, G.P. Tegos, H. Gali, T.Wharton, T. Sarna, M.R. Hamblin. Photodynamic therapy with fullerenes. *Photochem. Photobio. Sci.* **6**, 1139 (2007).
8. S. Afreen, K. Muthoosamy, S. Manickam, U.Hashim. Functionalized fullerene (C_{60}) as a potential nanomediator in the fabrication of highly sensitive biosensors. *Biosens. Bioelectron.* **63,** 354 (2015).
9. S. Pfuetzner, J. Meiss, A. Petrich, M. Riede, K. Leo. Improved bulk heterojunction organic solar cells employing C_{70} fullerenes. *Appl. Phys. Lett.* **94**, 223307 (2009).
10. H. Ajie, M. M. Alvarez, S. J. Anz, R.D. Beck, F. Diederich, K. Fostiropoulos, D.R. Kraetschmer, M. Rubin, K.E. Schriver, D. Sensharma, R.L. Whetten. Characterization of the soluble all-carbon molecules C_{60} and C_{70}. *J. Phys. Chem.* **94**, 8630 (1990).
11. W. Krätschmer, L. Lamb, K. Fostiropoulos, D. R. Huffman. Solid C_{60}: a new form of carbon. *Nature* **347**, 354 (1990).
12. S. Leach, M. Vervloet, A. Despres, E.Breheret, J.P. Hare, T.J. Dennis, H.W. Kroto, R. Taylor, D.R.M. Walton. Electronic spectra and transitions of the fullerene C_{60}. *Chem. Phys.* **160**, 451 (1992).
13. S. Mochizuki, M. Sasaki, R. Ruppin. An optical study on C_{60} vapour, microcrystal beam and film. *J. Phys.: Condens. Matter* **10**, 2347 (1998).
14. J. Hora, P. Panek, K. Navratil, B. Handlirova, J. Humlicek, H. Sitter, D. Stifter. Optical response of C_{60} thin films and solutions. *Phys. Rev. B* **54**, 5106 (1996).
15. W. Zhou, S. Xie, S. Qian, T. Zhou, R. Zhao, G. Wang, L. Quian, W. Li. Optical absorption spectra of C_{70} thin films. *J. Appl. Phys.* **80**, 459 (1996).
16. G. Orlandi, F. Negri. Electronic states and transitions in C_{60} and C_{70} fullerenes. *Photochem. Photobio. Sci.* **1**, 289 (2002).
17. R.C. Haddon, L.E. Brus, K. Ragnavachari. Electronic structure and bonding in icosahedral C_{60}. *Chem. Phys. Lett.* **125**, 459 (1986).
18. S. Saito, A. Oshiyama. Cohesive mechanism and energy bands of solid C_{60}. *Phys. Rev. Lett.* **66**, 2637 (1991).
19. V. Capozzi, G. Casamassima, G.F. Lorusso *et al.* Optical spectra and photoluminescence of C_{60} thin films. *Solid State Commun.* **98**, 853 (1996).
20. S. Kazaoui, N. Minami. Optical and electrical properties of C_{60}, C_{70}, nanotubes and endohedral fullerenes. In *Macromolecular Science and Engineering. Edited by Y. Tanabe* (Springer, 1999).

21. T. E. Saraswati, U. H. Setiawan, M. R. Ihsan, I. Isnaeni, Y. Herbani. The study of the optical properties of C_{60} fullerene in different organic solvents. *Open Chem.* **17**, 1198 (2019).
22. K. Yabana, G.F. Bertsch. Forbidden transitions in the absorption spectra of C_{60}. *Chem. Phys. Lett.* **197**, 32 (1992).
23. J.P. Hare, H.W. Kroto, R. Taylor. Preparation and 'UV/visible spectra of fullerenes C_{60} and C_{70}. *Chem. Phys. Lett.* **177**, 394 (1991).
24. G.E. Scuseria. The equilibrium structure of C_{70}. An ab initio Hartree-Fock study. *Chem. Phys. Lett.* **180**, 451 (1991).
25. J. Shumway, S. Satpathy. Polarization-dependent optical properties of C_{70}. *Chem. Phys. Lett.* **211**, 595 (1993).
26. R.E. Stratmann, G.E. Scuseria1, M.J. Frisch. Density functional study of the infrared vibrational spectra of C_{70}. *J. Raman Spectrosc.* **29,** 483 (1998).

Received 11.05.23.
Translated from Ukrainian by O.I. Voitenko

М.П. Горішний

МОРФОЛОГІЯ ПОВЕРХНІ ПЛІВОК СУМІШІ ФУЛЕРЕНІВ C_{60}/C_{70}. ІДЕНТИФІКАЦІЯ C_{60} ТА C_{70} У ПЛІВКАХ C_{60}/C_{70} ЗА ЇХ СПЕКТРАМИ ПОГЛИНАННЯ

Плівки суміші C_{60}/C_{70} наносили на різні підкладинки методом термічної сублімації у вакуумі 6,5 мПа. Досліджено морфологію поверхні плівок C_{60}/C_{70} товщиною 195 нм. Встановлено, що на кремнеземних і мідних підкладинках формуються полікристалічні і квазіаморфні плівки C_{60}/C_{70}, відповідно. Природа смуг поглинання C_{60} і C_{70} була детально обговорена на основі аналізу літератури та наших даних. Спектри поглинання плівок C_{60}, C_{70} і суміші C_{60}/C_{70} описувалися сумою функцій Гауса. Смуги поглинання C_{60} (2,474, 3,440 і 3,640 еВ) і C_{70} (2,594, 2,804, 3,018 і 3,252 еВ) можуть бути використані для ідентифікації цих речовин у сумішах фулеренів. Було виявлено, що C_{60} є домінуючим компонентом у плівках C_{60}/C_{70}.

Ключові слова: тонка плівка, морфологія поверхні, спектри поглинання, підгонка, Гаусіани, суміш C_{60}/C_{70}.